In vitro evaluation of the imaging accuracy of C-arm conebeam CT in cerebral perfusion imaging

A. Ganguly[a)]
Department of Radiology, Stanford University, Stanford, California 94305

A. Fieselmann
Pattern Recognition Lab, Department of Computer Science, Friedrich-Alexander University Erlangen-Nuremberg, 91058 Erlangen, Germany; Erlangen Graduate School in Advanced Optical Technologies (SAOT), Friedrich-Alexander University Erlangen-Nuremberg, 91058 Erlangen, Germany; and Siemens AG, Healthcare Sector, 91301 Forchheim, Germany

J. Boese
Siemens AG, Healthcare Sector, 91301 Forchheim, Germany

C. Rohkohl
Pattern Recognition Lab, Dept of Computer Science, Friedrich-Alexander University Erlangen-Nuremberg, 91058 Erlangen, Germany and Siemens AG, Healthcare Sector, 91301 Forchheim, Germany

J. Hornegger
Pattern Recognition Lab, Department of Computer Science, Friedrich-Alexander University Erlangen-Nuremberg, 91058 Erlangen, Germany and Erlangen Graduate School in Advanced Optical Technologies (SAOT), Friedrich-Alexander University Erlangen-Nuremberg, 91058 Erlangen, Germany

R. Fahrig
Department of Radiology, Stanford University, Stanford, California 94305

(Received 30 March 2012; revised 10 August 2012; accepted for publication 17 September 2012; published 12 October 2012)

Purpose: The authors have developed a method to enable cerebral perfusion CT imaging using C-arm based conebeam CT (CBCT). This allows intraprocedural monitoring of brain perfusion during treatment of stroke. Briefly, the technique consists of acquiring multiple scans (each scan comprised of six sweeps) acquired at different time delays with respect to the start of the x-ray contrast agent injection. The projections are then reconstructed into angular blocks and interpolated at desired time points. The authors have previously demonstrated its feasibility *in vivo* using an animal model. In this paper, the authors describe an *in vitro* technique to evaluate the accuracy of their method for measuring the relevant temporal signals.

Methods: The authors' evaluation method is based on the concept that any temporal signal can be represented by a Fourier series of weighted sinusoids. A sinusoidal phantom was developed by varying the concentration of iodine as successive steps of a sine wave. Each step corresponding to a different dilution of iodine contrast solution contained in partitions along a cylinder. By translating the phantom along the axis at different velocities, sinusoidal signals at different frequencies were generated. Using their image acquisition and reconstruction algorithm, these sinusoidal signals were imaged with a C-arm system and the 3D volumes were reconstructed. The average value in a slice was plotted as a function of time. The phantom was also imaged using a clinical CT system with 0.5 s rotation. C-arm CBCT results using 6, 3, 2, and 1 scan sequences were compared to those obtained using CT. Data were compared for linear velocities of the phantom ranging from 0.6 to 1 cm/s. This covers the temporal frequencies up to 0.16 Hz corresponding to a frequency range within which 99% of the spectral energy for all temporal signals in cerebral perfusion imaging is contained.

Results: The errors in measurement of temporal frequencies are mostly below 2% for all multiscan sequences. For single scan sequences, the errors increase sharply beyond 0.10 Hz. The amplitude errors increase with frequency and with decrease in the number of scans used.

Conclusions: Our multiscan perfusion CT approach allows low errors in signal frequency measurement. Increasing the number of scans reduces the amplitude errors. A two-scan sequence appears to offer the best compromise between accuracy and the associated total x-ray and iodine dose.
 [http://dx.doi.org/10.1118/1.4757910]

Key words: perfusion CT, C-arm, conebeam CT, interventional imaging, x-ray, arterial input function, venous input function, sinusoid

I. INTRODUCTION

Cerebral perfusion CT is an important imaging tool for diagnosis and therapy planning in stroke.[1] For acute ischemic stroke cases presented within 3 h from symptom onset, intravenous (IV) drug delivery remains the primary treatment of choice.[2–4] However, there is an increase in the use of endovascular approaches[5] for treatment. These approaches allow extension of the treatment time window and may reduce or eliminate the risk of symptomatic hemorrhage that could result from the use of thrombolytic drugs. However, the delay between CT scan acquisition and the time to the start of the image-guided endovascular intervention is significant with reported average delays of 1.4 (Ref. 6) to 5.3 h.[7] Major changes in the brain perfusion status can occur during the delay window.[5] Hence, availability of perfusion CT scans on imaging systems used for guiding endovascular procedures could have a significant impact on outcome by allowing perfusion monitoring pre-, intra-, and postprocedure, more accurate determination of procedure endpoint, and confirmation of tissue reperfusion.

We have previously demonstrated the feasibility of performing cerebral perfusion CT using a C-arm based conebeam CT (CBCT) system.[8] Typically such systems are optimized to provide fluoroscopic and angiographic guidance during endovascular procedures. More recently, they have also been enabled for volumetric imaging. However, the rotational speeds (∼4 s per 200°) are much slower compared to clinical CT scanners (0.33–0.5 s per 360°). Our previously reported work describes acquisition of accurate quantitative cerebral perfusion parameters in healthy swine imaged using such a C-arm CT system.[8] A special image acquisition and reconstruction algorithm developed for this purpose and early *in vitro* work using a quantitative evaluation of the new acquisition and reconstruction algorithm is described in subsequent publications.[9–11] In the current paper, we present more extensive *in vitro* evaluations and comparison using CT images as the gold standard. An improved phantom that allows higher resolution data sampling compared to our earlier reported version[12] was used for this study. These studies evaluate the temporal resolution of the imaging system in the context of cerebral perfusion CT.

Perfusion calculations involve imaging the time-density curves (TDC) of intravascular iodinated contrast and analyzing enhancement HU values on a voxel-by-voxel basis to quantify the blood flow, volume, and transit times.[13–15] The iodinated contrast agent serves as a radio-opaque surrogate for blood. To eliminate any influence of the contrast bolus injection on the tissue perfusion, the arterial input function (AIF) is removed from the data through deconvolution. While the tissue TDCs have wide peaks, the AIFs have sharper peaks requiring higher sampling rates for accurate representation. Hence, the ability of a system to accurately measure the AIF, in particular its high frequency components, should provide a measure for the suitability of the system for perfusion CT. This study looks at the fidelity with which the various temporal frequencies are imaged on a C-arm CT system in conjunction with the modified imaging and reconstruction protocol.

In order to have a simple and practical way to evaluate the temporal resolution, we developed a phantom that uses multiple compartments each filled with different dilutions of iodinated contrast. We did not measure the imaging accuracy of our system by imaging the AIF directly as has been described in the literature.[16] This would limit the measurements to one or maybe a few representative AIF curves, therefore, limiting the scope of the study only to those datasets. For a more generalized approach, we analyzed the accuracy with which each temporal frequency can be imaged, using the fact that the Fourier decomposition of any signal consists of weighted sinusoids of various frequencies also called the Fourier series. By evaluating the energy content and calculating the frequency below which most of the energy of the signal is contained, the relevant maximum frequency to be imaged can be determined. Hence, by creating a sinusoidal phantom that can generate various temporal frequencies, we can quantify the temporal accuracy of the imaging system. A disc phantom with sinusoidally varying iodine contrast concentrations based on similar arguments has been simulated by Montes *et al.*[17,18] While their phantom simulates inplane temporal frequencies, our phantom studies time varying signal perpendicular to the image slice. This is more relevant in cerebral perfusion since often the AIF is measured in a blood vessel that is perpendicular to the image slice. Below we describe the latest version of the phantom and the measurements performed to quantify the temporal accuracy of the imaging and reconstruction algorithm.

II. MATERIALS AND METHOD

II.A. Imaging considerations

The parameters for the phantom construction and imaging were based on perfusion results from the animal study that we have reported on recently.[8] The signal requiring the highest temporal resolution and in most cases the highest HU value is the AIF. Excluding an outlier, the average peak AIF signal level recorded for our animal studies was 780 ± 168 HU with the maximum value of 1009 HU. Hence, the desired peak signal for the phantom was set to 1000 HU while designing the phantom. The Fourier transform of the AIF and its energy density for various frequencies was used to choose the highest frequencies that needed to be replicated by the phantom. This is described below.

Cerebral AIF is most commonly represented mathematically as a gamma-variate function of the form[13,14,19,20]

$$c(t) = \frac{A(t-t_0)^a}{(a\cdot b\cdot e^{-1})^a} e^{-(t-t_0)/b} u(t-t_0), \quad (1)$$

where A is the peak enhancement, a and b are shape parameters, and $u(t-t_0)$ is a step function that is nonzero only at $t > t_0$. As per the literature, the variable a has a value of 3 and the variable b is 1.5 or 1 for IV and intra-arterial (IA) injections, respectively. Clinical CT scans use IV injection of contrast. However in the C-arm setting we have chosen to use an IA approach.[8] Primarily this approach was chosen to improve signal-to-noise ratio (SNR) thereby allowing lower

volumes of iodine contrast to be used per scan. For the animal studies conducted with an intra-arterial approach, a b value of approximately 2 gave the closest match to the model AIF.

The relative spectral energy density as a function of frequency is given by the integral squared modulus of the Fourier transform (FT) of the original AIF signal. This is evaluated as follows at $t_0 = 0$:

$$C(f) = FT\left[\frac{At^a}{(a\cdot b\cdot e^{-1})^a}e^{-t/b}u(t)\right] = \frac{A}{(a\cdot b\cdot e^{-1})^a}\int_0^\infty t^a e^{-t/b}e^{-2\pi i f t}dt. \quad (2)$$

Using known solutions for definite integrals, the FT expression has an analytical solution of the form

$$C(f) = \frac{A}{(a\cdot b\cdot e^{-1})^a}\cdot\frac{\Gamma(a+1)}{(1/b+2\pi i f)^{(a+1)}}. \quad (3)$$

From the squared modulus of the amplitude of this solution, the spectral energy density $E(f)$ can be evaluated as

$$E(f) = |C(f)|^2 = CC^+ = \left(\frac{A\Gamma(a+1)}{(a\cdot b\cdot e^{-1})^a}\right)^2\cdot\frac{1}{(1/b^2+4\pi f^2)^{(a+1)}}. \quad (4)$$

The AIF for the IV and IA injections that fit the model described in Eq. (1) and the corresponding accumulated spectral energy density as a function of temporal frequency $f$are shown in Figs. 1(a) and 1(b).

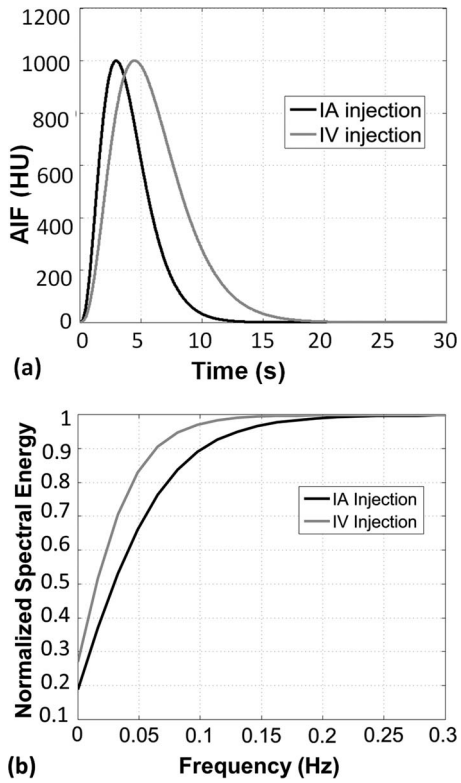

FIG. 1. Plots showing (a) the AIF for an arterial and a venous injections (b) normalized accumulated spectral energy as a function of sinusoid frequency (95% accumulated energy is contained within 0.10 Hz for arterial and 0.06 Hz for venous injection.

From the accumulated energy density spectrum we can see that 90% of the power in the AIF spectrum is contained below 0.06 Hz (or 95% below 0.10 Hz) for gamma-variate signal with $b = 1$ and 90% of the power is below 0.1 Hz for $b = 2$. In fact, data from sample human CT scans have been shown to contain 90% of the spectral energy lies within 0.06 Hz for IV injections and up to 99% within 0.15 Hz even using a conservative estimate.[17] Given these numbers, the highest frequency targeted for the phantom was 0.16 Hz. This covers the range needed to evaluate the AIF from the various injections as well as allowing an analysis of the range of frequencies over which the fidelity is reproduced in images from the C-arm system.

II.B. Phantom construction

A cylindrical phantom was machined from an acrylic tube of 1.9 cm inner diameter and divided into compartments of 0.5 cm height. The total length of the phantom was 32.2 cm resulting in 64 compartments. The partitions were separated using a thin sheet of carbon fiber that was 0.5 mm thick to minimize the sudden change in contrast between successive compartments containing different volumes of iodinated contrast. Each compartment had a single opening through which the contrast was injected using a syringe.

To create the sinusoidal signal, the contrast concentrations in successive compartments were prepared such that the resulting opacification in the reconstructed x-ray image has a sinusoidal variation in HU numbers. The relative intensities were chosen to represent values corresponding to (1 + sin θ) resulting in a minimum relative value of 0 and a maximum of 2. This circumvents the problem of negative values of the *sine* function that cannot be generated using iodine contrast agent and water mixture. Using the linearity curve obtained for different concentrations of iodinated contrast (300 mgI/Omnipaque; Nycomed, Princeton, NJ),[11] the amounts necessary to satisfy the relative and peak intensities were determined. The peak concentration of the contrast agent was adjusted to result in a value of ~1000 HU. This value was selected since the maximum AIF value encountered during a previously reported animal study had a maximum of 1009 HU. The corresponding iodine contrast concentration range was 0%–7%. Intermediate concentrations were adjusted so that a total of five complete sinusoids were accommodated within the length of the phantom. The phantom was placed within the bore of a 15 cm diameter cylindrical jacket of water approximating the attenuation of the head. The imaging setup is shown in Fig. 2(a).

II.C. Phantom setup and verification

II.C.1. Iodine concentration verification

The inherent errors in the preparation of the iodinated solutions and the HU accuracy of the images obtained from the C-arm CT system were evaluated. Test tubes each filled with 40 ml of the prepared solutions at the various concentrations were imaged using the C-arm system and the clinical CT

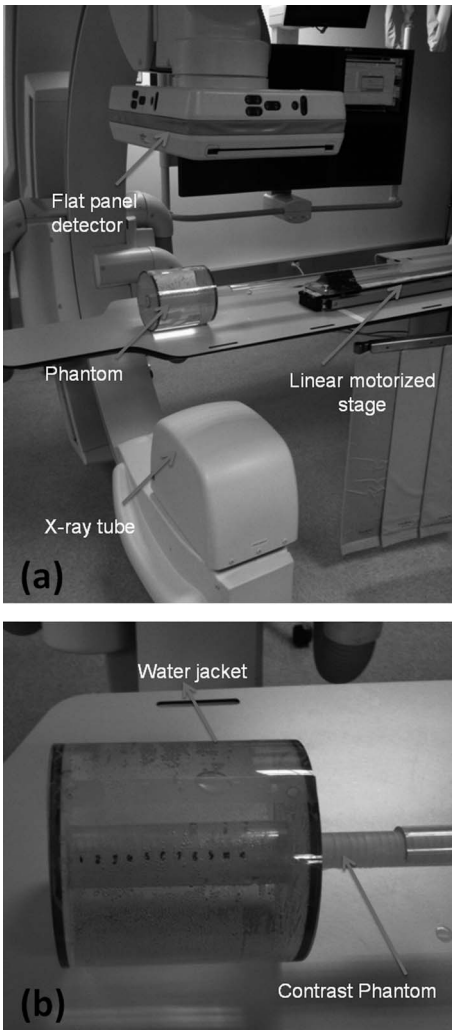

FIG. 2. (a) Imaging setup for C-arm CT imaging of the phantom (b) Closeup image of contrast agent phantom contained within a water jacket.

system. The values obtained from the clinical CT data were used as a gold standard.

II.C.2. Phantom motion

The phantom was mounted on a motorized linear stage (Parker Motors Model, Parker Hannifin Corp., OH) and moved along the rotation axis parallel to the patient table (z-axis) of the imaging system [Fig. 2(b)]. When observed from a single location in the laboratory frame of reference, the sinusoidal phantom moving at velocity v results in a sinusoid of frequency given by the following equation:

$$F(t) = B\sin[2\pi f t + F(0)] + \varphi_0. \quad (5)$$

Here, the frequency

$$f = \frac{\mathrm{v}}{\lambda} \quad (6)$$

with the wavelength

$$\lambda = \frac{L}{n}, \quad (7)$$

where $L = 32.2$ cm is the length of the phantom and $n = 5$ is the number of complete wavelengths in the phantom. The amplitude of the signal is given by B and the initial phase by φ_0. To analyze the temporal resolution of the reconstructed image using the special acquisition and reconstruction scheme developed, data were acquired at different values of the linear velocity from 0.1 to 1.0 cm/s in steps of 0.1 cm/s resulting in sinusoidal frequencies of approximately 0.02–0.16 Hz.

II.D. Clinical CT imaging

CT images were acquired on a clinical system (Discovery, GE Medical Systems, Waukesha, WI) every 0.5 s at 80 kVp. The CT noise index value that determines the mA range during automated tube current modulation on these scanners[21] was set to 50 to provide reference images with high SNR. This resulted in an average mA value of 400 for each scan. The acquisition slice thickness was set to 1.25 mm. To evaluate the HU values of the prepared iodinate solutions, test tubes containing 40 ml of the 7 different iodine concentrations were imaged. Images of the moving phantom were then acquired for the sinusoidal frequency measurements. The linear stage with the phantom was placed along the central axis of the clinical CT system. Images of the phantom were obtained with the phantom moving at speeds of 0.5–1.0 cm/s in steps of 0.1 cm/s for each scan and corresponding to a sinusoid frequency range of 0.075–0.16 Hz. Imaging at lower frequencies was unnecessary as explained in the discussion (see Sec. II.D).

II.E. C-arm CT imaging

A C-arm CT imaging system (Siemens Axiom Artis dTA and syngo DynaCT^{TM}, Siemens AG, Healthcare Sector, Forchheim, Germany) was used for the study. The linear stage with the phantom was set up with the axis of motion along the z-axis of the system and passing through the isocenter [Fig. 2(a)]. To ensure alignment of the translational axis, fluoroscopic test images from orthogonal directions were obtained as the phantom traveled along the z-axis. A single frame in each view was analyzed to ensure that the phantom axis passed through the center of the image frame.

For the actual CBCT, imaging was performed at 81 kVp using 6 sets of scans (each containing 6 bidirectional sweeps of 4.2 s) at each linear velocity setting. At the start of each sweep, the following offsets to the start of phantom linear motion were used: −4.6, −2.8, −0.9, 0.9, 2.8, and 4.6 s with negative delays representing delay to the start of a contrast injection and positive delay referring to delay to start of imaging. We have described this modified imaging technique that allows improvement in temporal resolution in other publications[8,10] and the basic idea is depicted in Fig. 3. In our phantom study, there is no actual flow of iodinated contrast from an injector. Hence, the inject delays were replaced by delays to the start of translation of the phantom. This was encoded within the software program for driving the phantom's linear stage. The x-ray delays on the other hand were implemented using the injector interface (Medtron AG,

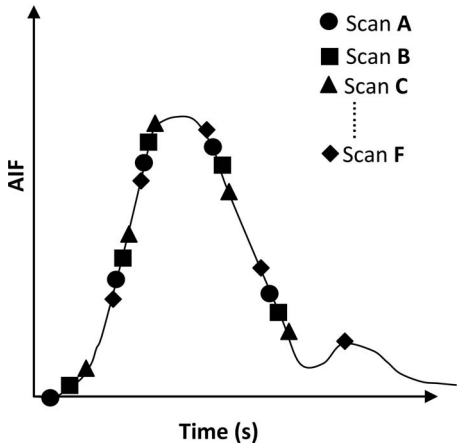

FIG. 3. Staggered image acquisition scheme for obtaining improved sampling of data using the C-arm CT system. Each scan set (denoted by letters A though F) indicates a different delay between start of injection and image acquisition.

Saarbrücken, Germany) that allows synchronization with the C-arm system.

II.F. Image reconstruction

The CT images were reconstructed with voxel size of 0.39 × 0.39 × 5 mm^3. The C-arm CT data were reconstructed using the specially developed interpolation technique involving partial block backprojection (PBB).[1,8–10,20] The reconstruction voxel size was 0.5 × 0.5 × 0.5 mm^3 from which 5 mm slices were obtained during postprocessing. Briefly, the PBB reconstruction process involves dividing the data from each sweep into six equiangular blocks. Each block is backprojected and data for each voxel is interpolated temporally between blocks. It is assumed that the change in attenuation values of the voxels in a block are negligible over the time required to scan the block. Linear interpolation is then used to generate complete reconstructed data at intervals of 1 s.

As mentioned above, a dataset for a given velocity consisted of six scans with different delays. Each scan in turn consists of six bidirectional sweeps. We denote each scan with the letters A through F with A representing the scan with −4.6 s delay and so on. Hence, a six-injection scan set would be denoted by A-B-C-D-E-F. For the animal study that we reported, we looked at the feasibility of using fewer than the entire set of six scans. Fewer scans would mean lower volume of iodine contrast injected, lower x-ray exposure and shorter study time. Though a single injection followed by a scan set would be ideal, the resulting cerebral blood flow (CBF) maps from the animal study were not as accurate. Hence, we analyzed the best candidate sequences which were the following: B-D-F, A-C, and B-D in addition to the A-B-C-D-E-F sequence. In the current study, we also looked at single injection-and-scan options: A, B, and C to quantify the degradation in performance. From the acquired dataset, the above mentioned subsets were reconstructed and the frequency of the resulting sinusoid was compared to the calculated values and to the results from the CT reconstruction.

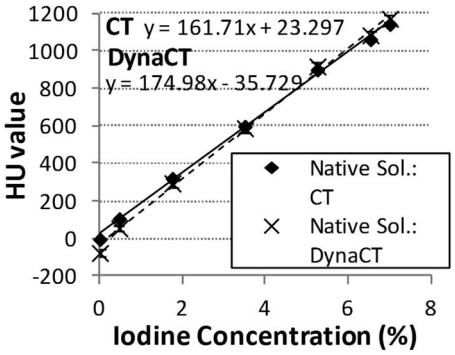

FIG. 4. Linearity curve for the clinical CT and C-arm CT system obtained using test tubes of iodine contrast agent at concentrations used in the subsequent phantom experiments.

II.G. Image analysis

The HU value in a 10 × 10 pixel region-of-interest (ROI) centered in the middle of the starting slice of the reconstructed CT volume was averaged. The average value in the ROI for all subsequent slices passing through this ROI as the phantom moves in time was recorded. This average HU value was measured in all the relevant slices for both C-arm CT and CT data, for all the cases analyzed. A sinusoid of the form in Eq. (5) was fitted to the data in each case. The least-squared best fit curve was used to fit the experimental data. The value of the sinusoid frequency obtained from fitting the C-arm CT data was compared to the mathematically calculated value obtained from Eq. (6) for a given velocity v and also compared to the sinusoid frequency that fit the CT data.

III. RESULTS

III.A. Iodine concentration verification

Figure 4 shows the linearity of the HU values measured for the native iodinated contrast solutions prepared for use in the phantom. The linear fit to the data shows that the difference in the slopes of the HU vs iodine concentration for data acquired on the clinical CT and C-arm CT scanner differ by 8%. The differences are more pronounced at the low HU values and tend to agree best at midrange values at around 600 HU.

While the maximum HU value for these solutions when imaged in the test tube is ∼1100 HU, the peak value reduces to about ∼1000 HU when the solutions are poured into the phantom compartments and the phantom is placed in the 15 cm water jacket for final imaging. This can be seen in Fig. 5 where the results of imaging the sinusoidal phantom using the clinical CT scanner are plotted. The peak to peak value for all frequencies of the sinusoid imaged on the CT scanner has an average value of 1021.34 ± 1.07 HU which is 10.64% lower than the peak CT value of the native iodine contrast and water mixtures.

Once the differences in the CT values between the two imaging systems were established for the static phantom, the HU values for moving phantom were compared. Figures 6 and 7 show the results of imaging using the C-arm conebeam CT system in conjunction with the specialized image processing and reconstruction method. Figure 6 displays the decreasing

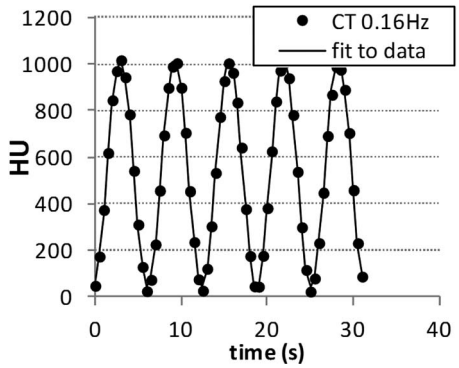

FIG. 5. Result of clinical CT imaging of sinusoidal-contrast phantom moving at 10 cm/s or equivalently imaging a sinusoid of 0.16 Hz.

accuracy in imaging the sinusoids as their frequency increases and aliasing sets in. Sample illustrative cases with the sinusoid frequency ranging from 0.12 to 0.16 Hz are shown. The results in this figure are for the best case scenario which uses all six sets of scans or the A-B-C-D-E-F sequence.

As can be expected, the resulting inaccuracies increase as the number of scan sets used decreases due to increased aliasing. The most dramatic change occurs when two scans sets are used instead of a single set. An example of scan set dependence is shown in Fig. 7, illustrating the result of using various scan combinations at a sinusoid frequency of 0.09 Hz. While the frequency match for the six scan set as well as the two and three scan sets is within 2% of the ground truth, the errors in the amplitude measurement are more pronounced as the number of scans is reduced.

The measurement errors are shown in Figs. 8 and 9. The amplitude error (Fig. 8) measures the error between the peak to peak value of the sinusoids and the maximum CT signal of the native solution (shown in Fig. 4). The errors in amplitude measurements of the moving phantom in the clinical CT data and the C-arm data are shown. The amplitude errors increase with increasing frequency for all the C-arm CT scans with the errors going up as the number of scan sets used is reduced. The errors in frequency measurement (Fig. 9) on the other hand remain fairly flat at below ~2% for most of the scan sets but increase dramatically for the single scan (A, B, and C) sets above 0.10 Hz. The error plots could be used to find an optimal balance between the required accuracy for perfusion imaging and the x-ray and iodine dose to be delivered.

IV. DISCUSSION

Small differences in the absolute value of the CT numbers exist between clinical CT and C-arm CT using a 4 s scan even for the static scans. This is evident in Fig. 4 where the linear fits to the data show slightly different slopes and intercept and further manifest as HU errors particularly as amplitude inaccuracies. The overall effect of the amplitude errors will result in different absolute values of the AIF and TDC. Real physiological data is comprised of multiple frequencies with the AIF having more of the higher values in the range and the TDC having primarily most of the lower frequencies. Hence, the errors will be in accordance with the weighting of different frequency components in the AIF and TDC spectra. For the actual calculation of the perfusion parameters, the

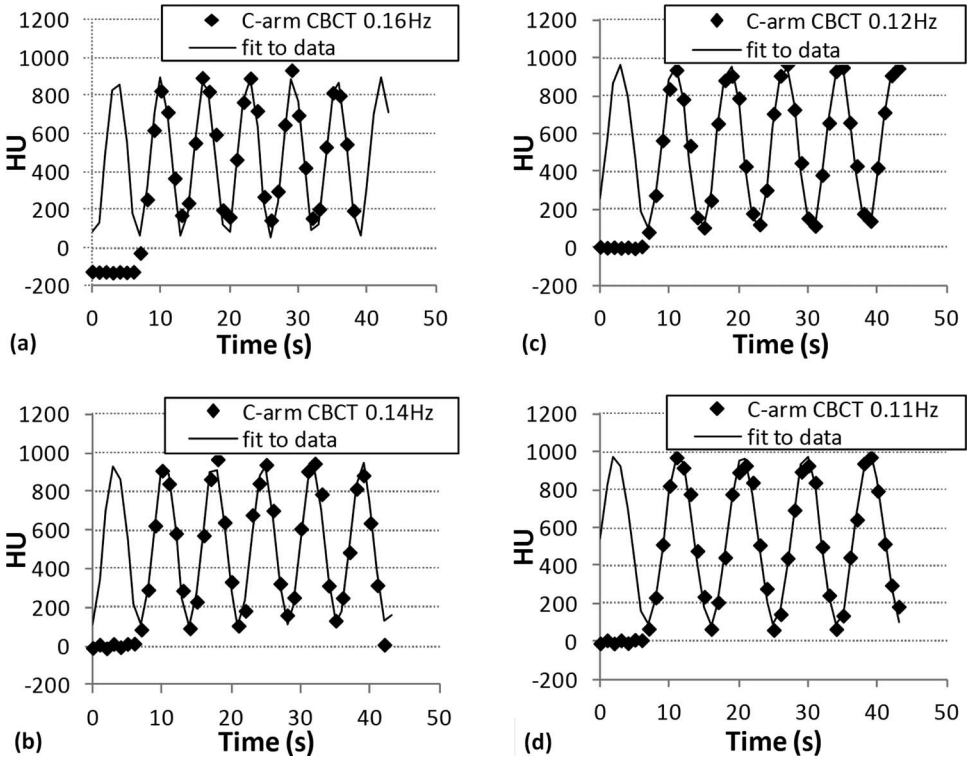

FIG. 6. Result of C-arm CT imaging of sinusoidal-contrast phantom moving at velocities 1–0.7 cm/s (a)–(d) or equivalently imaging of sinusoid of 1–0.7 Hz. These results are for the A-B-C-D-E-F scan set.

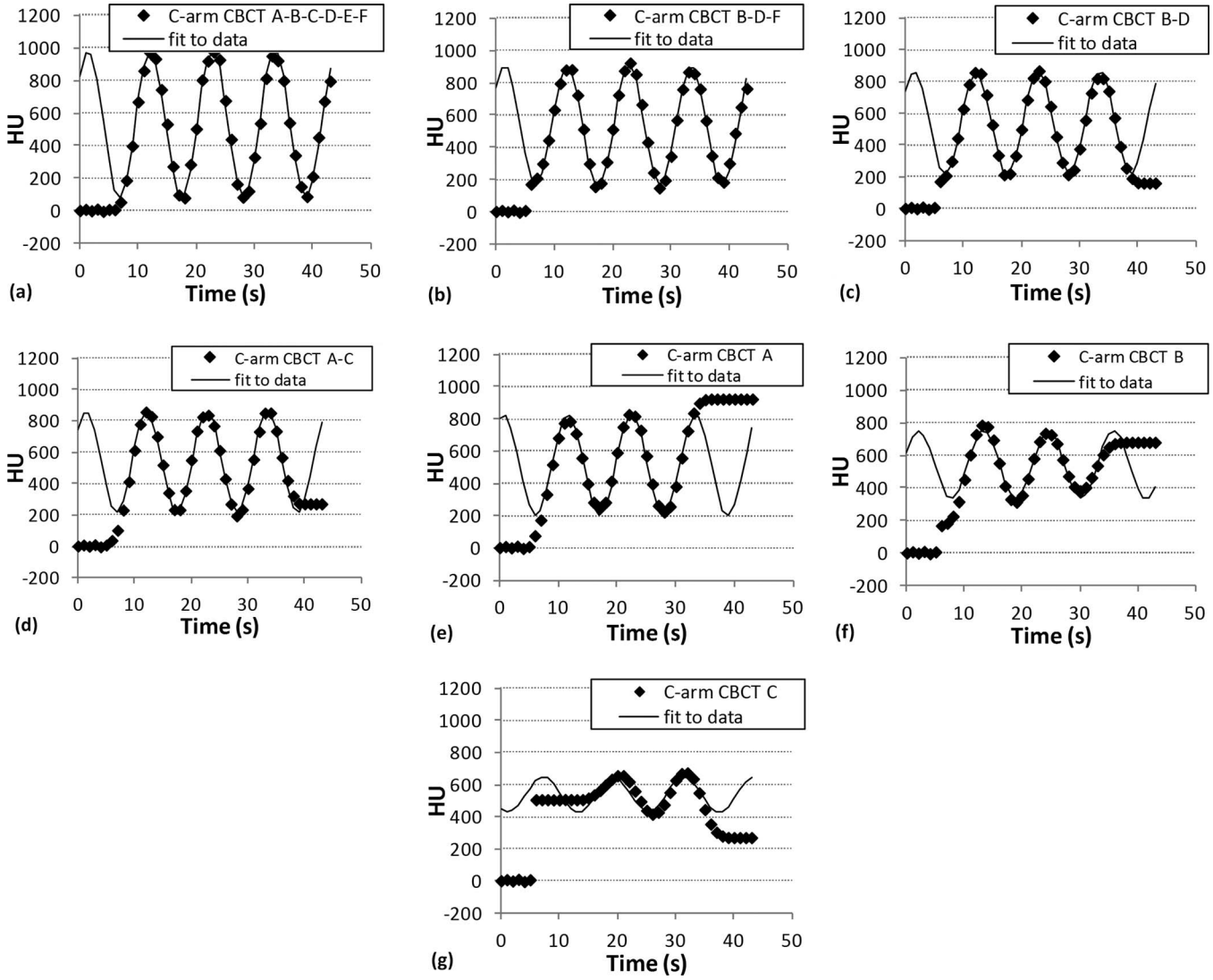

FIG. 7. Results of C-arm CT scans at 0.6 cm/s or 0.09 Hz for different number of scan set combination (a)–(g). Errors increase as the number of scans used is reduced.

tissue HU values are normalized by the AIF values. This normalization will improve the accuracy of the final perfusion parameters although the actual TDC values and AIF will have errors depending on the number of scan sets used. However, when the TDC values are very low and noisy, this advantage could be reduced.

The errors in the mechanical setup depend on the accuracy of the motor in the linear stage and in the three-dimensional alignment of the axis of motion. To ensure that the phantom always traveled along the axis passing through the isocenter and parallel to the patient table, orthogonal projection images

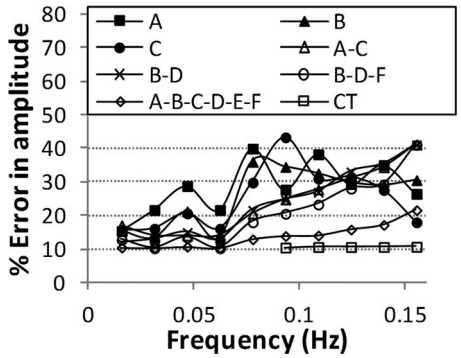

FIG. 8. Error in measurement of the frequencies of the various sinusoids.

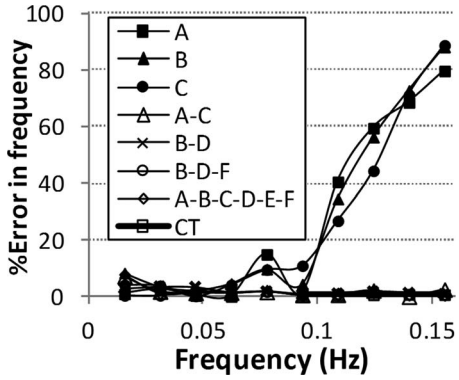

FIG. 9. Error in peak-to-peak amplitude measurement of the sinusoids from 0.02 to 0.16 Hz.

were used. In each row, the darkest pixel corresponding to the thickest part of the iodine-containing cylinder was assessed to ensure alignment with the center of the image. The accuracy for this technique is within 2 pixel widths or 388 μm.

The linear stage has an accuracy of 0.001 mm/s. This corresponds to the accuracy of the velocities of travel for the sinusoid or equivalently a temporal frequency accuracy of 15.5 μHz.

While the design of the phantom and the experiments are sufficient to evaluate the C-arm CT system, difficulties are encountered when imaging on the clinical CT system. At lower velocities ($\leq$0.5 cm/s or equivalently $\leq$0.078 Hz), the partition between the successive compartments causes CT numbers to drop due to partial volume effects when the partition is present in the imaging slice. The data show discrete periodic jumps, and results in data distributions that are difficult to fit to the sinusoidal curve of Eq. (5). Hence, CT data at velocities $<$0.6 cm/s were not used in the study. There was also sufficient fidelity in the higher frequency results on CT as seen in Fig. 5 to allow a safe assumption that the lower frequencies would be replicated accurately.

The simple phantom reported here and the concept of imaging sinusoids of different frequencies can be applied more generally for assessing imaging temporal resolution. By analyzing the spectral energy, the relevant range of sinusoid frequencies to be imaged can be determined.

V. CONCLUSIONS

The above experiments indicate that using the C-arm CT system, a single scan set could be sufficient for imaging signals with temporal frequency content of 0.06 Hz and below. This conclusion assumes that there is sufficient SNR in the reconstructed slices particularly in the case of imaging in stroke applications. For higher temporal frequencies, inclusion of at least one more scan set improves results dramatically. Although using six scan sets has the best outcome with respect to amplitude accuracy, use of two scan sets could provide the needed compromise between accuracy and x-ray dose, iodinated contrast dose, total imaging time, and complexity.

ACKNOWLEDGMENTS

This work was supported by a research grant from Siemens AG, Healthcare Sector, Forcheim, Germany. Financial support to some of the authors was also provided by the following sources: National Institutes of Health Grant No. K99 EB007676, the Lucas Foundation, and the Erlangen Graduate School in Advanced Optical Technologies (SAOT) by the German Research Foundation (DFG) in the framework of the German excellence initiative.

[a]Author to whom correspondence should be addressed. Electronic mail: Arun.Ganguly@varian.com

[1]H. P. J. Adams *et al.*, "Guidelines for the early management of adults with ischemic stroke: A guideline from the American Heart Association/American Stroke Association Stroke Council, Clinical Cardiology Council, Cardiovascular Radiology and Stroke Council, Clinical Cardiology Council, Cardiovascular Radiology and Intervention Council, and the Atherosclerotic Peripheral Vascular Disease and Quality of Care Outcomes in Research Interdisciplinary Working Groups: The American Academy of Neurology affirms the value of this guideline as an educational tool for neurologists," Stroke **38**, 1655–1711 (2007).

[2]K. A. Miles, "Measurement of tissue perfusion by dynamic computed tomography," Br. J. Radiol. **64**(761), 409–412 (1991).

[3]K. A. Miles, M. Hayball, and A. K. Dixon, "Colour perfusion imaging: A new application of computed tomography," Lancet **337**(8742), 643–645 (1991).

[4]M. Wintermark, R. Sincic, D. Sridhar, and J. D. Chien, "Cerebral perfusion CT: Technique and clinical applications," J. Neuroradiol. **35**(5), 253–260 (2008).

[5]G. M. Nesbit, G. Luh, R. Tien, and S. L. Barnwell, "New and future endovascular treatment strategies for acute ischemic stroke," J. Vasc. Interv. Radiol. **15**(1 Pt 2), S103–S110 (2004).

[6]K. Nedeltchev *et al.*, "Pre- and in-hospital delays from stroke onset to intra-arterial thrombolysis," Stroke **34**(5), 1230–1234 (2003).

[7]A. J. Furlan and A. Abou-Chebl "The role of recombinant pro-urokinase (r-pro-UK) and intra-arterial thrombolysis in acute ischaemic stroke: The PROACT trials. Prolyse in acute cerebral thromboembolism," Curr. Med. Res. Opin. **18**(suppl 2), s44–s47 (2002).

[8]A. Ganguly *et al.*, "Cerebral CT perfusion using an interventional C-arm imaging system: Cerebral blood flow measurements," AJNR Am. J. Neuroradiol. **32**(8), 1525–1531 (2011).

[9]A. Fieselmann, "Interventional perfusion imaging using C-arm computed tomography: Algorithms and clinical evaluation," Ph.D dissertation, Friedrich-Alexander University of Erlangen-Nuremberg, Erlangen-Nuremberg, Germany, 2011.

[10]A. Fieselmann, F. Dennerlein, Y. Deuerling-Zheng, J. Boese, R. Fahrig, and J. Hornegger, "A model for filtered backprojection reconstruction artifacts due to time-varying attenuation values in perfusion C-arm CT," Phys. Med. Biol. **56**(12), 3701–3717 (2011).

[11]A. Fieselmann, A. Ganguly, D-Z. Yu, J. Boese, R. Fahrig, and J. Hornegger, "Using a C-arm CT for interventional perfusion imaging: A phantom study to measure linearity between iodine concentration and Hounsfield values," presented at the Annual Meeting DGMP, Freiburg i. Br., Germany, 2010.

[12]A. Ganguly, A. Fieselmann, J. Boese, C. Rohkohl, J. Hornegger, and R. Fahrig, "Evaluating the feasibility of C-arm CT for brain perfusion imaging: An *in vitro* study," in *SPIE Physics of Medical Imaging* (SPIE, San Diego, 2010), p. 76250K-1–76250K-8.

[13]L. Ostergaard, A. G. Sorensen, K. K. Kwong, R. M. Weisskoff, C. Gyldensted, and B. R. Rosen, "High resolution measurement of cerebral blood flow using intravascular tracer bolus passages. Part II: Experimental comparison and preliminary results," Magn. Reson. Med. **36**(5), 726–736 (1996).

[14]L. Ostergaard, R. M. Weisskoff, D. A. Chesler, C. Gyldensted, and B. R. Rosen, "High resolution measurement of cerebral blood flow using intravascular tracer bolus passages. Part I: Mathematical approach and statistical analysis," Magn. Reson. Med. **36**(5), 715–725 (1996).

[15]A. Fieselmann, M. Kowarschik, A. Ganguly, J. Hornegger, and R. Fahrig, "Deconvolution-based CT and MR brain perfusion measurement: Theoretical model revisited and practical implementation details," Int. J. Biomed. Imaging **2011**, 467563 (2011).

[16]R. Brauweiler, F. Eisa, and W. Kalendar, "A dedicated perfusion phantom for validation of dose reduction techniques in dynamic CT," in *Proceedings of the Radiological Society of North America, Chicago, 2010* (Radiological Society of North America, Chicago, IL, 2010), p. SSK16-02.

[17]P. Montes, "Dynamic cone-beam reconstruction for perfusion computed tomography," Ph.D dissertation, Ruprecht-Karls-Universitat, Heidelberg, 2006.

[18]P. Montes and G. Lauritsch, "A temporal interpolation approach for dynamic reconstruction in perfusion CT," Med. Phys. **34**(7), 3077–3092 (2007).

[19]M. Mischi, J. A. denBoer, and H. H. Korsten, "On the physical and stochastic representation of an indicator dilution curve as a gamma variate," Physiol. Meas. **29**(3), 281–294 (2008).

[20]A. Fieselmann *et al.*, "Interventional 4-D C-arm CT perfusion imaging using interleaved scanning and partial reconstruction interpolation," IEEE Trans. Med. Imaging **31**(4), 892–906 (2012).

[21]K. M. Kanal, B. K. Stewart, O. Kolokythas, and W. P. Shuman, "Impact of operator-selected image noise index and reconstruction slice thickness on patient radiation dose in 64-MDCT," AJR, Am. J. Roentgenol. **189**(1), 219–225 (2007).